Food Research International 155 (2022) 111095

Contents lists available at ScienceDirect

Food Research International

journal homepage: www.elsevier.com/locate/foodres

Stearic acid prevent alcohol-induced liver damage by regulating the gut microbiota

Wen Nie [a,b], Feiran Xu [a,b], Kai Zhou [a,b,c], Xiaoxiao Yang [a,b], Hui Zhou [a,b], Baocai Xu [a,b,*]

[a] School of Food and Biological Engineering, Hefei University of Technology, Hefei 230601, China
[b] Engineering Research Center of Bio-process, Ministry of Education, Hefei University of Technology, Hefei 230601, China
[c] Anhui QiangWang Flavouring Food Co., Ltd, Fuyang 236500, Anhui, China

ARTICLE INFO

Keywords:
Jinhua ham
Fatty acids
Gut microbiota
Alcohol-associated liver damage
Intestinal barrier

ABSTRACT

The pathological characteristics of alcohol-associated liver damage (ALD) mainly include liver lipid accumulation, which subsequently leads to alcohol-associated steatohepatitis, fibrosis and cirrhosis. Dietary factors such as alcohol and fat may contribute to the development of ALD. A chronic alcohol-fed mouse model was used to investigate the effect of fatty acids in Jinhua ham on ALD. The fatty acids in Jinhua ham could prevent the occurrence of ALD from chronic alcohol consumption. In addition, the fatty acids in Jinhua ham with liver protective activity were long-chain saturated fatty acids (LCSFAs), including palmitic acid and stearic acid. In contrast, long-chain polyunsaturated fatty acids aggravated the pathogenesis of ALD. Furthermore, the mechanism underlying the prevention of ALD by fatty acids in Jinhua ham was ascribed to increasing relative abundances of *Akkermansia muciniphila* and *Lactobacillus* in the gut, which were beneficial to regulating intestinal homeostasis, ameliorating intestinal barrier dysfunction and reducing alcohol-associated hepatitis and oxidative stress damage. This study demonstrated that dietary supplementation with saturated fatty acids could prevent or mitigate ALD by regulating the gut microbiota (GM) and improving the intestinal barrier, while provided a more affordable dietary intervention strategy for the prevention of ALD.

1. Introduction

Alcohol-associated liver damage (ALD) is one of the most prevalent and preventable chronic diseases and is associated with severe morbidity and mortality worldwide. It includes a spectrum of the pathological characteristics of liver lipid accumulation, which subsequently leads to alcohol-associated steatohepatitis, alcohol fibrosis and cirrhosis (Gao & Bataller, 2011). The mortality from ALD count reaches approximately 2.5 million annually, with a mortality rate of 4% worldwide (Room, Babor, & Rehm, 2005). In Europe, ALD accounts for more than 75% of cirrhosis cases (Rehm, Shield, Rehm, Gmel, & Frick, 2012). Due to a lack of pharmacologic options for managing ALD, treatment of ALD remains a major health problem worldwide.

Alcohol is generally considered a highly diffusible small-molecule compound, with over 90% of alcohol being absorbed in blood circulation through the stomach and intestines after intake and subsequently being metabolized in the liver (Massey & Arteel, 2012; Norberg et al., 2003). Many toxic metabolites of alcohol are produced and accumulated in the liver, such as acetaldehyde and reactive oxygen species (ROS), which are responsible for disrupting intestinal barrier function and oxidative stress-mediated damage of hepatocytes (Arthur, 2006). Moreover, excessive alcohol consumption contributes to abnormal lipid

Abbreviations: AhR, aryl hydrocarbon receptor; ALD, alcohol-associated liver disease; ALT, alanine transaminase; AMPK, Adenosine 5'-monophosphate (AMP)-activated protein kinase; AST, aspartate transaminase; *CD14*, cluster of differentiation 14; CPT1, Carnitine palmityl transferase-1; CTRL, control group; *CYP2E1*, cytochrome P4502E1; ELISA, enzyme-linked immunosorbent assay; EtOH + JHF, sample group; EtOH, ethanol group; *FAS*, fatty acid synthase; GM, gut microbiota; GSH-Px, glutathione peroxidase; HE, hematoxylin and eosin; HO-1, heme oxygenase 1; IL-1β, interleukin-1β; IL-6, interleukin-6; JHF, fat in Jinhua ham; LPS, lipopolysaccharide; *MCP-1*, monocyte chemoattractant protein-1; *MD-2*, myeloid differential protein-2; MDA, malondialdehyde; *MyD88*, myeloid differentiation primary response 88; *NF-kB*, nuclear factor-k-gene binding; *NQO1*, (NAD(P)H:quinone oxidoreductase 1; *NRF2*, nuclear factor E2; PBS, phosphate-buffered saline; PPAR-α, peroxisome proliferators-activated receptors; ROS, reactive oxygen species; *SCD1*, stearoyl-CoA desaturase 1; SOD, superoxide dismutase; *SREBP1c*, sterol regulatory element binding protein 1c; TG, triglyceride; *TLR-4*, toll-like receptor 4; TNF-α, tumor necrosis factor α; RT-PCR, reverse transcription-polymerase chain reaction.

* Corresponding author at: School of Food and Biological Engineering, Hefei University of Technology, Hefei 230601, China.
E-mail address: baocaixu@163.com (B. Xu).

https://doi.org/10.1016/j.foodres.2022.111095
Received 12 January 2022; Received in revised form 1 March 2022; Accepted 2 March 2022
Available online 5 March 2022

metabolism in the liver by activating the signaling pathways of *SREBP1c* and *PPAR-α* (Crabb & Liangpunsakul, 2006). *SREBP1c* is a pivotal nuclear transcription factor in liver lipid metabolism, regulating liver lipid synthesis by regulating the expression of enzymes related to lipid metabolism, such as fatty acid synthase and stearoyl-CoA desaturase (You, 2002). The accumulation of acetaldehyde and TNF can upregulate the expression of the *SREBP1c* gene and accelerate its maturation in hepatocytes (Endo, Masaki, & Seike, 2007). Conversely, *PPAR-α* plays a beneficial role in preventing and ameliorating alcohol-induced lipid accumulation in the liver by promoting fatty acid β oxidation and export (Nakajima, Kamijo, Tanaka, Sugiyama, & Aoyama, 2010). *AMPK* plays a central role in alcohol-induced liver lipid metabolism abnormalities because it directly regulates the expression of the *SREBP1c* and *PPAR-α* genes (Brice, Julien, & Pedro, 2013; Molina, 2008).

The gut microbiota (GM) contributing to the pathogenesis of ALD has been clearly established (Albillos, de Gottardi, & Rescigno, 2020). Alcohol and its metabolite acetaldehyde can directly damage the intestinal barrier and disrupt intestinal homeostasis (gut bacterial overgrowth and dysbiosis), which worsens ALD (Yan et al., 2011). Intestinal barrier dysfunction leads to increased intestinal permeability, which promotes bacterial translocation and lipopolysaccharide (LPS) absorption (Sarin, Pande, & Schnabl, 2019). LPS, as an innate immunomodulator, participates in signaling with TLR4 and its coreceptors to stimulate the release of inflammatory cytokines by Kupffer cells, leading to hepatitis and scarring of liver tissue (Louvet & Mathurin, 2015).

Recent evidence has indicated that alcohol and the type of dietary fat are directly associated with the development of ALD (Irina, Matthew, Matthew, Swati, & Craig, 2016; Nanji & Frcnch, 1986). A large amount of experimental evidences suggested that dietary tuna fish oil, α-linolenic acid, eicosapentaenoic acid and docosahexaenoic acid exhibit potential therapeutic efficacy against ALD (Huang et al., 2013; Pawlosky, Flynn, & Salem, 1997; Pawlosky & Salem, 2004; Song, Moon, Olsson, & Salem, 2008; Wada, Yamazaki, Kawano, Miura, & Ezaki, 2008). However, several studies have demonstrated that dietary alcohol with corn oil resulted in more severe ALD than alcohol alone in experimental animals (Nanji et al., 1989, 1995). Moreover, dietary alcohol with menhaden fish oil aggravated the pathology of liver lipid accumulation and hepatitis to a greater extent than alcohol with corn oil (Nanji et al., 1994). Simultaneously, several investigators have indicated that treatment with palm oil and beef fat but not fish oil was associated with a marked improvement in ALD (Feng, Ma, & Wang, 2020; Nanji, Sadrzadeh, & Yang, 2010). The results regarding the role of specific types of dietary fat in ALD are still inconsistent and controversial.

Our previous study confirmed that dry-cured hams can prevent ALD, which is related to the bioactive peptides in dry-cured hams (Nie et al., 2020). However, the effect of the fat in dry-cured hams on ALD remains unclear. Therefore, the aim of the present study was to investigate the probable impacts of dry-cured ham fat on ALD and clarify the mechanism underlying the potentiation or attenuation of ALD. Clarifying the impact of the types of dietary fat on ALD and understanding the molecular mechanisms underlying the prevention of ALD development may help to provide a more affordable dietary intervention strategy for the prevention of alcohol-associated liver injury.

2. Materials and methods

2.1. Materials and chemicals

Jinhua hams (36-month ripening period) were obtained from the Jinzi Ham Food Company (Jinhua, Zhejiang, China). Casein 30 Mesh, L-cystine, corn starch, maltodextrin, sucrose, t-butylhydroquinone, mineral mix S10022G, vitamin mix V10037, choline bitartrate, cellulose, stearic acid (C18:0), palmitic acid (16:0), oleic acid (C18:1) and linoleic acid (C18:2) were of food grade and obtained from Hefei Yili Co., Ltd. (Hefei, Anhui, China). Corn oil was obtained from Yihai Kerry Golden Arowana Grain, Oil and Foodstuffs Co., Ltd. All the water used in this study was deionized water. The primer sequences of the targeted genes were showed in Supporting Information 1. Main antibodies TLR4, CD14, MyD88, MD-2, NF-kB, SREBP1c, SCD1, FAS, AMPK, PPAR-α, CPT1, CYP2E1, AhR, NQO1, Claudin-1 and Occludin were bought from Abcam (MA, USA), and antibodies against GAPDH were obtained from Sigma-Aldrich (USA). The secondary anti-rabbit IgG (H + L) and anti-mouse IgG (H + L) were obtained from Cell Signaling Technology (Beverly, MA, USA).

2.2. Extraction of fatty acid and preparation of the mouse diet

100 g Jinhua ham was homogenized with 500 mL petroleum ether by a polytron homogenizer (IKA T25 digital ultraturrox, IKA, Germany; 4 S, 10 s each at 15,000 rpm with cooling in ice). Then, the mixture was subjected to ultrasonic treatment for 1 h. The homogenate was centrifuged at 3500g for 20 min at 4 °C, and the filtered liquid was dried at 55 °C by a reduced pressure rotary evaporator. Finally, the fat retained in the rotary steaming bottle was the fat of Jinhua ham and used to prepare the mouse diet (Supporting Information 2 for the specific formula).

2.3. Animal experiments

The male SPF C57BL/6 mice (8 weeks old, weight 20 ± 2 g) used in this study were provided by Changzhou Kavins Experimental Animal Co. (license no.: SCXK (Su) 202106212). The mice were reared in a standard environment with a 12-hour alternating darkness/light cycle, and ad libitum to autoclaved food and distilled water. The ambient temperature was 25 ± 2 °C, and the relative humidity was 60 ± 5%. Animal experiments were performed according to the guidelines of the institutional animal ethics committee and were approved by the biomedical ethics committee of Hefei University of Technology (HFUT 20201026001). All mice were fed one week in advance for acclimation to the experimental environment.

The chronic alcohol-fed mouse model was established as previously described (Bertola, Mathews, Ki, Wang, & Gao, 2013). The mice were randomly divided into different groups (8 per group), including the control group, alcohol group, and experimental group, and fed for 35 days. The alcohol group was fed an EtOH diet with daily oral gavage of 3.0 g/kg B.W. alcohol from the 1th to the 14th day and 5.0 g/kg B.W. alcohol from the 15th to the 35th (EtOH group, n = 8). The control group was fed the CTRL diet with oral gavage of 5.4 g/kg B.W. maltose dextrin from the 1th to the 14th day and 9.0 g/kg B. W. maltose dextrin from 15th to the 35th (CTRL group, n = 8). The control group mice were fed an isocaloric amount of maltose dextrin instead of alcohol by oral gavage to maintain the same caloric intake (1 g of ethanol = 7 kcal; 1 g of maltose dextrin (Bio-serv) = 3.89 kcal). The experimental group was fed a JHF/C16:0/C18:0/C18:1/C18:2/C18:3 diet (where JHF is the fat in Jinhua ham) with oral gavage of 3.0 g/kg B.W. alcohol from the 1th to the 14th day and 5.0 g/kg B.W. alcohol from the 15th to the 35th (JHF/C16:0/ C18:0/C18:1/C18:2 + EtOH group, n = 8). The details of the animal feeding strategy are described in Fig. 1. Nine hours after the final gavage, all mice were euthanized in a CO_2 chamber, followed by collection of serum, liver, colon and intestinal contents.

2.4. Fatty acid analysis

Fatty acid methyl esters were analyzed by gas chromatography (Daglioglu, Tasan, & Tuncel, 2000). Approximately 10 g of sample was weighed, and 25 mL of hexane was added to the centrifuge tube. Then, the mixture was subjected to ultrasonic treatment for 20 min. The supernatant was collected after centrifugation (3500*g* for 10 min at 4 °C). The hexane was removed by rotary evaporation at 55 °C for 10 min, and 20 μL of the acquired oil, 400 μL of KOH/methanol (1 mol/L) and 2 mL of hexane were added to a 10 mL centrifuge tube and lightly vortexed. Then, 2 mL of ultrapure water was added, and the mixture was placed at

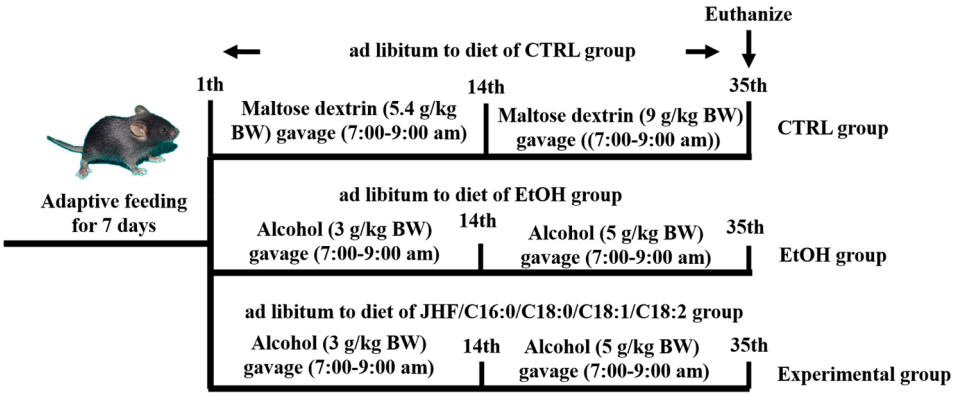

Fig. 1. Experimental design for the protocol used for ALD in male C57BL/6J mice.

room temperature for separation. Finally, 1 mL of the supernatant was collected and filtered through a 0.22-μm membrane filter. A gas chromatograph (Agilent Technologies, USA) with a DB-WAX capillary column (30 m × 0.25 mm × 0.25 μm) was used to monitor the composition of fatty acids with the following parameter settings: injector temperature: 270 °C; detector temperature: 280 °C; programmed temperature conditions: initial temperature of 100 °C for 13 min, heating from 100 to 180 °C at 10 °C/min, holding for 6 min, heating from 180 to 200 °C at 1 °C/min, holding for 20 min, heating from 200 to 230 °C at 4 °C/min, holding for 10.5 min; carrier gas: nitrogen; split ratio: 100:1; injection volume: 1 μL.

2.5. Serum, feces and liver biochemical analysis

The blood supernatant in the anticoagulant tube was collected after centrifugation (1500*g* for 10 min at 4 °C) as serum. The alanine transaminase (ALT), aspartate transaminase (AST) and triglyceride (TG) levels in serum were determined according to the kit instructions; 1 g of feces was taken, and 2 mL of normal saline was added to homogenize the samples in an ice bath environment. Then, the samples were centrifuged at 3000*g* at 4 °C for 10 min, and the supernatant was taken to determine the TG level; 1 g of liver tissue was taken and cut into pieces, and then, 5 mL of precooled normal saline was added to homogenize the liver tissue in an ice bath environment. Then, the supernatant was centrifuged at 3000*g* at 4 °C for 10 min, and the levels of alcohol dehydrogenase (ADH), acetaldehyde dehydrogenase (ALDH), malondialdehyde (MDA), TG, superoxide dismutase (SOD), and glutathione peroxidase (GSH-Px) and protein were determined. The levels of all the above indicators were determined according to commercial kits according to the manufacturer's instructions (Nanjing Jiancheng Bioengineering Institute, Nanjing, China).

2.6. Histopathological analyses

Liver/colon tissue was immobilized in a 4% paraformaldehyde solution. The fixed tissue was embedded in paraffin, sliced into 5-μm slices, and stained with hematoxylin-eosin/Alcian blue solution. Each stained section was placed on a slide and observed under an optical microscope.

2.7. Analysis of inflammatory cytokines in the liver

One gram of liver tissue was taken and cut into pieces, and then, 5 mL of precooled normal saline was added to homogenize the liver tissue in an ice bath environment. Then, the supernatant was centrifuged at 3000*g* at 4 °C for 10 min. The levels of LPS, TNF-α, IL-1β and IL-6 were determined by enzyme-linked immunosorbent assay (ELISA) kits obtained from Jiangsu Mei Biao Biological Technology Co., Ltd. (Yanchen, Jiangsu, China), and the protein concentrations were determined by a BCA protein assay kit (Nanjing Jiancheng Bioengineering Institute, Nanjing, China).

2.8. Analysis of the GM

Bacterial metagenomes from colon content samples were extracted using an Omega EZNA™ fecal genome extraction kit according to the manufacturer's instructions. The extracted total DNA samples were quantitatively analyzed by a NanoDrop 1000 nucleic acid concentration analyzer and qualitatively examined by 1% agarose gel electrophoresis. Samples that met the sequencing requirements (DNA concentration >50 ng/μL, with clear bands) were stored in a −80 °C freezer for future use. The structure of the GM was analyzed based on the V3-V4 variable region of the bacterial 16S rRNA gene according to the literature (Nie et al., 2021). F338 (5′-ACTCCTACGGGAGGCAGCAGCAG-3′) and R806 (5′-GGACTACHVGGGTWTCTAAT-3′) were used as primers to amplify the V3-V4 variable region of the 16S rRNA gene in the bacterial genome. The amplicon libraries were built to the required data depth using the library building kit, and then, on the Illumina MiSeq PE300 platform, paired-end sequencing was performed at 2 × 300 bp by Suzhou BioNovo Gene Co., Ltd. The original data have been submitted to the NCBI database. The BioProject number is PRJNA772101.

2.9. RNA extraction and real-time fluorescence quantitative PCR analysis

Total RNA was extracted from the liver and colon by TRIzol Reagent (Invitrogen, Carlsbad, CA) and subjected to concentration determination (NanoDrop 2000, Thermo Fisher, USA). Then, cDNA was synthesized by using a high-capacity cDNA reverse transcription kit (Applied Biosystems, Foster City, CA). All primers for quantitative analysis of expression were designed by Primer Premier 5 software according to the gene sequence in NCBI. Real-time quantitative polymerase chain reaction (RT-PCR) was performed on a Heal Force CG-02 thermocycler (Heal Force, China) with PowerUp SYBR Green Master Mix (Applied Biosystems, Foster City, CA). All the samples were prepared in triplicate. After standardization to the *GAPDH* expression level, duplicate samples were measured to calculate the relative levels of target genes. Relative mRNA expression was calculated using the $2^{-\Delta\Delta Ct}$ method.

2.10. Western blot analysis

The liver or colon tissues were washed with cold PBS and cut into fragments. Then, the fragments were homogenized with PMSF at a final concentration of 1 mM to form a tissue homogenate. Then, with a ratio of 200 μL of RIPA buffer per 60 mg of tissue, RIPA buffer was added to the tissue homogenate for lysing cells in an ice bath environment for 15 min. The supernatant of the tissue homogenate was collected after centrifugation (2000*g* for 5 min at 4 °C) as cytoplasmic protein. The concentration of the nondenatured protein solution was measured with

a BCA protein assay kit (Nanjing Jiancheng Bioengineering Institute, Nanjing, China). The 5× reduced gel sample loading buffer was added to the protein solution at a ratio of 4:1, and the mixture was heated in a boiling water bath for 15 min. Then, SDS-PAGE (concentrating gel voltage: 75 V, separating gel voltage: 120 V) was performed until the bromophenol blue indicator was approximately 1 cm from the bottom, at which point the electrophoresis was terminated. The proteins on the gel were transferred to polyvinylidene difluoride membranes (Servicebio, Wuhan, China). The membranes were quickly washed in an incubation tank filled with TBST and blocked with 5% skim milk at room temperature for 30 min. Primary antibodies were added, and the membranes were incubated at 4 °C in a shaker overnight. Then, the membranes were washed with TBST (three times, 5 min each). The secondary antibody was diluted with TBST at a ratio of 1:5000 and then added to the membranes for incubation at room temperature for 30 min. Finally, western blotting was performed by using an ECL chemiluminescence kit (Thermo Scientific, CA, USA). ImageJ software (NIH, USA) was used for densitometric analysis of the bands.

2.11. Statistical analysis

All experiments were repeated at least three times. The results are expressed as the mean ± S.E.M. Significant differences among all groups were calculated according to one-way ANOVA followed by the Bonferroni post hoc test. The differences in species diversity between groups were analyzed by a T-test. Linear discriminant analysis effect size (LEfSe) was used to compare two or more groups and identify significantly different biomarkers between groups.

3. Results and discussion

3.1. The effect of JHF on alcohol-induced liver damage

ALT, AST and MDA were identified as the main biomarkers of alcohol-introduced liver damage (Saravanan, Viswanathan, & Pugalendi, 2006). As shown in Fig. 2A-C, the levels of ALT, AST and MDA were 20.86 U/L, 98.49 U/L and 45.35 mmol/mL, respectively, in the CTRL group. After absolute alcohol treatment, the levels of ALT (130.19 U/L), AST (353.87 U/L) and MDA (203.02 mmol/mL) were significantly higher than those in the CTRL group ($P < 0.05$). The results demonstrated that the mouse model of alcohol-induced liver damage was successfully developed. When alcohol and JHF were administered simultaneously, the levels of ALT (63.18 U/L), AST (190.79 U/L) and MDA (122.28 mmol/mL) were significantly lower than those in the EtOH group ($P < 0.05$). These results indicated that JHF effectively ameliorated liver damage caused by alcohol consumption.

3.2. Effect of JHF characteristics on alcohol-induced liver damage

JHF is a complex containing a variety of fatty acids with different characteristics. To further identify the functional factors in JHF for ALD prevention, the differences in the fatty acid compositions of dietary lipids were compared and evaluated in this study. The percentages of palmitic (C16:0), stearic acid (C18:0) and oleic acid (C18:1) in JHF were significantly ($P < 0.05$) higher than those in corn oil, but the percentages of linoleic acid (C18:2) and linolenic acid (C18:3) in JHF were significantly ($P < 0.05$) lower than those in corn oil (Table 1). This may be the reason for the prevention of ALD by JHF. To further verify our hypothesis, the effects of individual fatty acids in JHF on ALD were separately investigated. The results showed that saturated fatty acids (C16:0 and C18:0) significantly ameliorated ALD, while unsaturated fatty acids, especially polyunsaturated fatty acids (C18:2 and C18:3), promoted the development of experimental ALD (Fig. 3A-C). We verified that dietary supplementation with palmitic acid (C16:0) and stearic acid (C18:0), which are saturated LCFAs, could prevent the development of ALD in mice. In addition, the group that received dietary supplementation with stearic acid (C18:0) showed stronger liver protection activity than the group that received dietary supplementation with palmitic acid (C16:0). In summary, the prevention of ALD by JHF was mainly attributed to it being rich in long-chain saturated fatty acids (LCSFAs), especially stearic acid. Interestingly, we found that with the same carbon chain, the greater the carbon double-bond content in fatty acids was, the more the development of ALD was promoted. The carbon chain length of fatty acids may also affect the course of ALD, but this part of the research is ongoing and will not be described here.

3.3. Effects of stearic acid on lipid absorption and alcohol metabolism

To further clarify the mechanism underlying the preventive effect of stearic acid on ALD, the effect of stearic acid on lipid absorption was investigated in this study. As shown in Fig. 4A, the levels of fecal TG in CTRL group, EtOH group and EtOH + stearic acid (C18:0) group were not significant difference between any two groups ($P > 0.05$). This suggested that the prevention of ALD by stearic acid was not associated

Table 1
Fatty acid compositions of corn oil and JHF.

Fatty acid	Percentage (%)	
	Corn oil	JHF
C14:0	trace	trace
C16:0	10.13 ± 1.24^{b}	32.17 ± 1.47^{a}
C16:1	trace	trace
C18:0	2.17 ± 0.25^{b}	19.97 ± 1.44^{a}
C18:1	26.73 ± 2.82^{b}	39.50 ± 1.73^{a}
C18:2	60.50 ± 2.27^{a}	8.36 ± 1.24^{b}
C18:3	0.74 ± 0.12	trace
∑SFA	12.3 ± 0.99^{b}	52.13 ± 2.78^{a}
∑USFA	87.7 ± 3.83^{a}	47.87 ± 1.65^{b}
SFA/USFA	0.139 ± 0.01^{b}	1.09 ± 0.12^{a}

Different letters (a, b) in the same line indicate significant differences ($P < 0.05$).

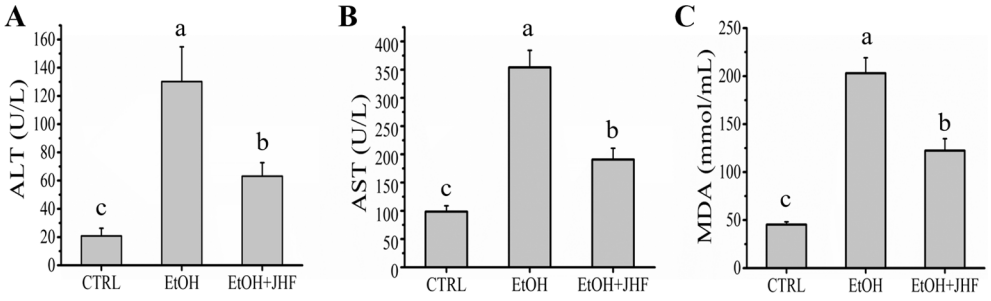

Fig. 2. Effects of JHF on serum concentrations of ALT (A), AST (B) and MDA (C) in male mice fed a control diet or an ethanol-containing diet with or without JHF for 35 days. Values are means ± S.E.M; n = 8. Samples designated with different lower cases letters (a, b, c) were significantly different ($P < 0.05$) when compared different treatment group.

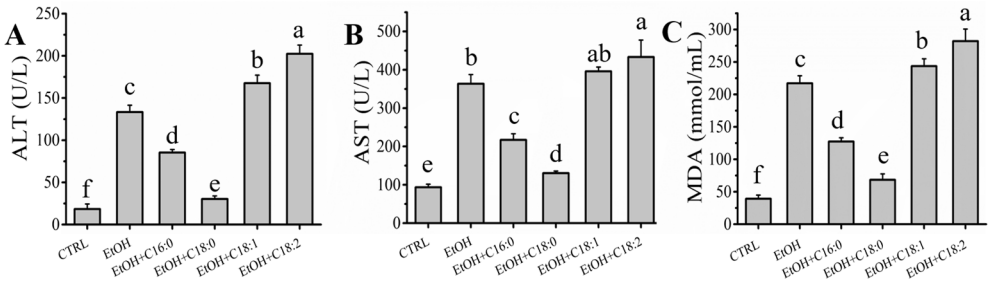

Fig. 3. Effects of single fatty acid in Jinhua hams on serum concentrations of ALT (A), AST (B) and MDA (C) in male mice fed a control diet or an ethanol-containing diet with or without different single fatty acids for 35 days. Values are means ± S.E.M; n = 8. Samples designated with different lower cases letters (a, b, c, d, e and f) were significantly different ($P < 0.05$) when compared different treatment group.

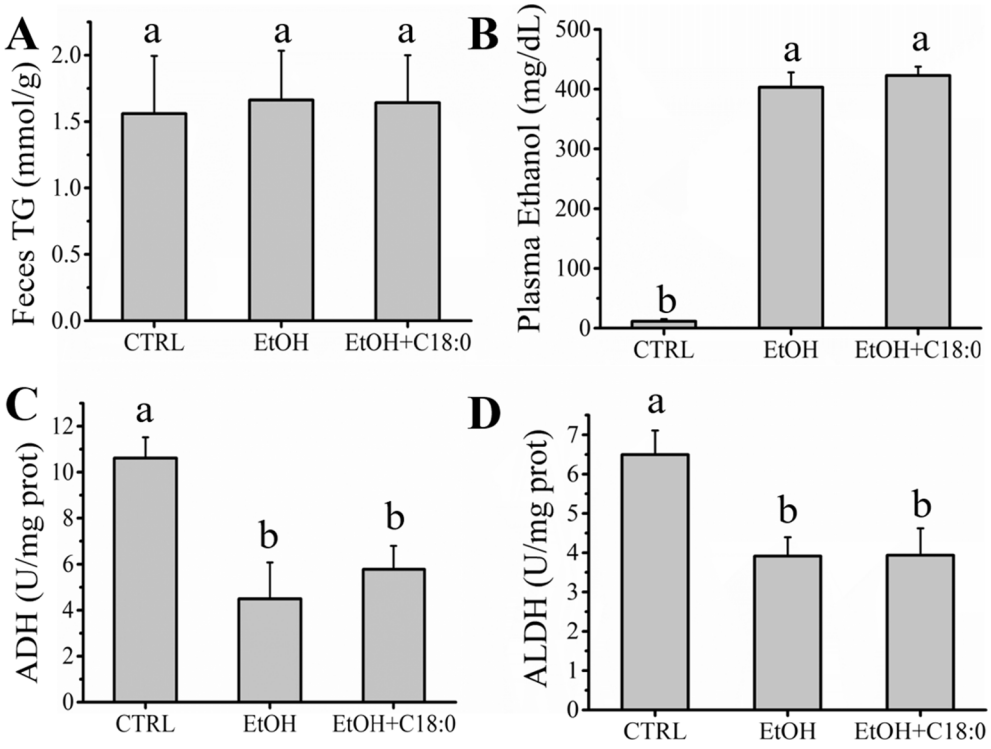

Fig. 4. (A) Effects of stearic acid (C18:0) on feces concentrations of TG; (B) Effects of stearic acid (C18:0) on plasma concentrations of ethanol; (C) Effects of stearic acid (C18:0) on liver activity of ADH; (D) Effects of stearic acid (C18:0) on liver activity of ALDH; Values are means ± S.E.M; n = 8. Samples designated with different lower cases letters (a, b) were significantly different ($P < 0.05$) when compared different treatment group.

with lipid absorption. The absorption of alcohol in the intestine and metabolism of alcohol in the liver are important factors for ALD. The absorption of alcohol was investigated by measuring the concentration of ethanol in plasma. As shown in Fig. 4B, the concentration of ethanol in plasma was significantly increased after alcohol consumption compared with that in the CTRL group ($P < 0.05$). However, the concentration of ethanol in plasma was similar between the EtOH + C18:0 group and EtOH group ($P > 0.05$) (Fig. 4B). This suggested that the prevention of ALD by stearic acid is not associated with the absorption of alcohol. ADH and ALDH are the main hepatic enzymes responsible for metabolizing alcohol. ADH is responsible for the dehydrogenation of alcohol to acetaldehyde, and ALDH converts acetaldehyde to acetic acid, which is finally broken down to CO_2 and H_2O for elimination (Xiao, Zhou, Zhao, Su, & Sun, 2018). In the CTRL group, the activities of ADH and ALDH were 10.62 U/mg prot and 6.49 U/mg prot, respectively. After alcohol administration, the activities of ADH (4.49 U/mg prot) and ALDH (3.91 U/mg prot) decreased significantly compared with those in the CTRL group ($P < 0.05$). However, stearic acid pretreatment did not significantly reverse this trend ($P > 0.05$). (Fig. 4C-D) This demonstrated that the mechanism underlying the preventive effect of stearic acid (C18:0) on ALD is not associated with hepatic metabolism of alcohol. A previous study found that alcohol consumption reduced the capacity of the GM to synthesize LCSFAs, resulting in a lack of LCSFAs in the gut (Peng, Torralba, Tan, Embree, & Schnabl, 2014). Therefore, it is reasonable to speculate that the mechanism underlying the preventive effect of stearic acid on ALD is related to the GM. However, the effects of saturated fatty acids on the composition of the GM and the molecular patterns associated with pathogens remain unclear.

3.4. Stearic acid changed the profiles of the GM in alcohol-treated mice

To verify the above conjecture, the effects of alcohol consumption and dietary supplementation with stearic acid on the profiles of the GM were investigated in this study. As shown in Fig. 5A, the GM consisted mainly of *Firmicutes*, *Verrucomicrobia* and *Bacteroidetes* at the phylum level. At the genus level, the proportions of *Akkermansia* and *Lactobacillus* were markedly decreased and that of *Lachnospiraceae_NK4A136* was significantly increased in the EtOH group, while stearic acid

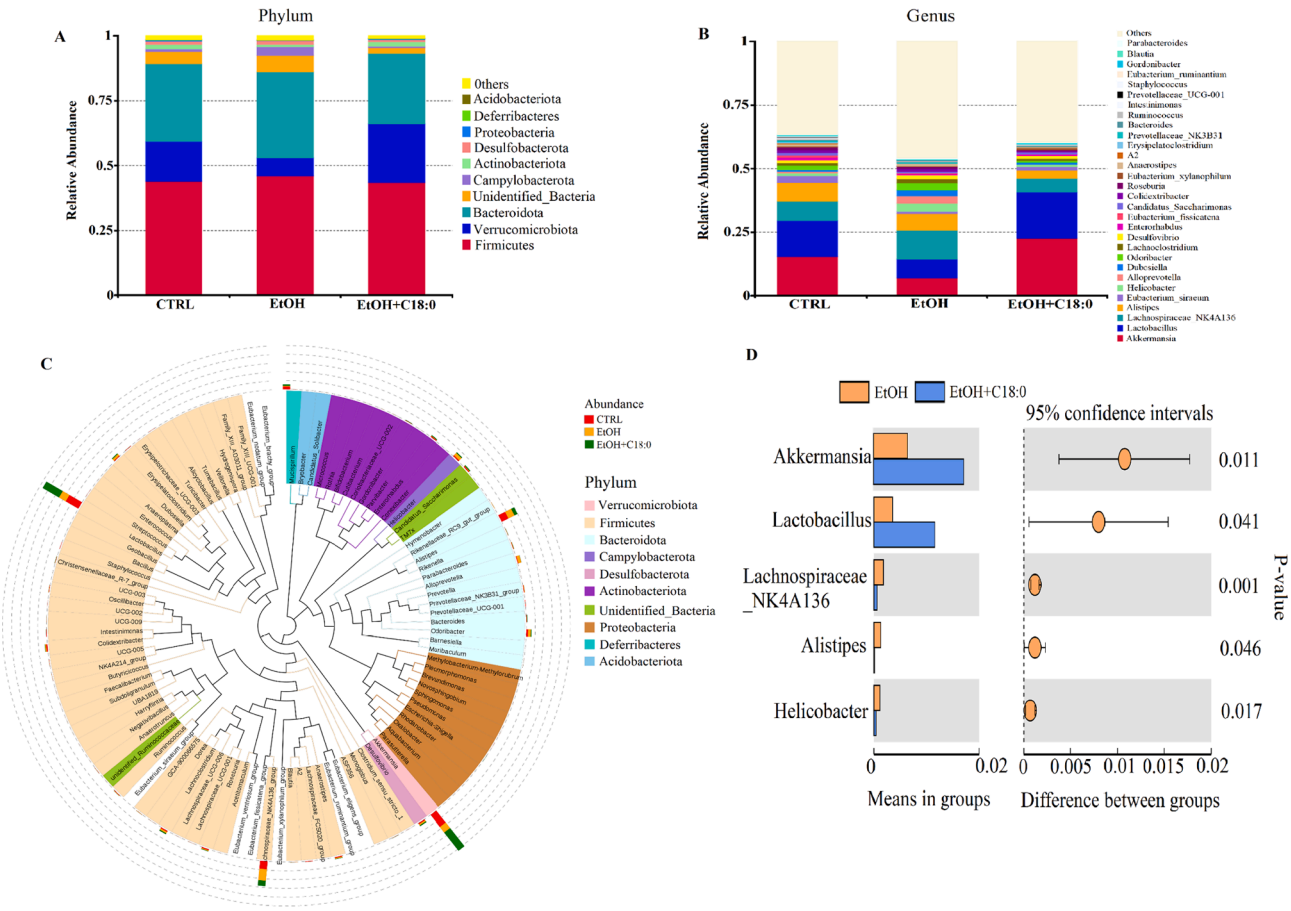

Fig. 5. (A) Effects of stearic acid (C18:0) on relative abundances of gut bacteria at phylum level. (B) Effects of stearic acid (C18:0) on relative abundances of gut bacteria at genus level. (C) Analysis of the differences of gut bacteria at phylum level in three dietary groups. (D) Analysis of the differences of gut bacteria at genus level in EtOH and EtOH + C18:0 group.

pretreatment significantly reversed these trends (Fig. 5B-D). The presently recognized pathogenic factors connecting intestinal dysbiosis and ALD appear to be bacterial and metabolite (e.g., LPS) translocation caused by increased intestinal permeability (Kirpich et al., 2013; Yan & Arthur, 2012). The factors behind the pathogenesis of the increased intestinal permeability are exposure to ethanol and acetaldehyde, which causes gut epithelial cell tight junction (TJ) disruption (Tremaroli & Bäckhed, 2012). Previous studies had confirmed that *Akkermansia* and *Lactobacillus* had the capacity to ameliorate alcohol-induced epithelial barrier function for preventing ALD by promoting intestinal mucosal wound regeneration and redox-mediated intestinal epithelial cell proliferation and migration (Hsieh, Chen, Kuo, & Ho, 2021; Liu et al., 2020; Macchione et al., 2019; Neyrinck et al., 2016; Xia et al., 2020). In this study, stearic acid pretreatment could prevent ALD by promoting the relative abundance of *Akkermansia* and *Lactobacillus* in the gut, which might improve alcohol-induced intestinal barrier dysfunction, enhance gut epithelial cell tight junction (TJ) and reduce the leakage of LPS.

3.5. Stearic acid improved intestinal epithelial barrier function in alcohol-treated mice

To further confirm above hypothesis, we investigated the effects of stearic acid and metabolites of gut microbiota (*Akkermansia* and *Lactobacillus*) on alcohol-induced intestinal barrier dysfunction. Mucus is an essential part of maintaining the health and functional integrity of the gastrointestinal tract. It represents both a first barrier that protects the epithelial surface, preventing penetration by bacteria or LPS, an excellent substrate and lubricant for bacterial growth, adhesion and metabolic processes (Cone, 2009). As shown in Fig. 6A, stearic acid (C18:0) alleviated alcohol-mediated deformation of enterocytes and reduction of intestinal mucous layer thickness, according to histopathological analysis of the colon. Moreover, the epithelial TJ protein is essential for maintaining the integrity of the intestinal barrier and influencing intestinal epithelial leakage (Grander et al., 2018). As shown in Fig. 6B-C, stearic acid ameliorated the alcohol-mediated reductions in the mRNA and protein expression levels of *claudin-1* and *occludin*. Reduced mucous layer formation and increased intestinal permeability are markers of intestinal barrier dysfunction, which results in LPS leaking into the liver through portal venous circulation, activating liver Kupffer cells and other immune cells to produce a large number of proinflammatory factors, leading to liver inflammation and damage (Szabo, 2015). These results demonstrated that stearic acid could ameliorate alcohol-mediated intestinal barrier dysfunction by increasing the thickness of the mucous layer and the epithelial TJ of the intestine.

However, whether stearic acid plays a direct role in ameliorating alcohol-induced intestinal epithelial barrier dysfunction is a question worthy of further investigation. Therefore, we investigated the effect of stearic acid on an alcohol-induced Caco-2 cell injury model in vitro (Supporting Information 3–4). With the increase of alcohol treatment concentration, the viability of Caco-2 cell were significantly ($P < 0.05$) lower than that of CTRL group (Fig. 6D). The viability of Caco-2 cell was about 47.38 ± 5.77% at the alcohol concentration of 300 mmol/L, which was the semi-lethal concentration of alcohol for Caco-2 cell (IC50). This result implied that the model of alcohol-induced Caco-2 cell damage had been established successfully. As demonstrated in Fig. 6E-G,

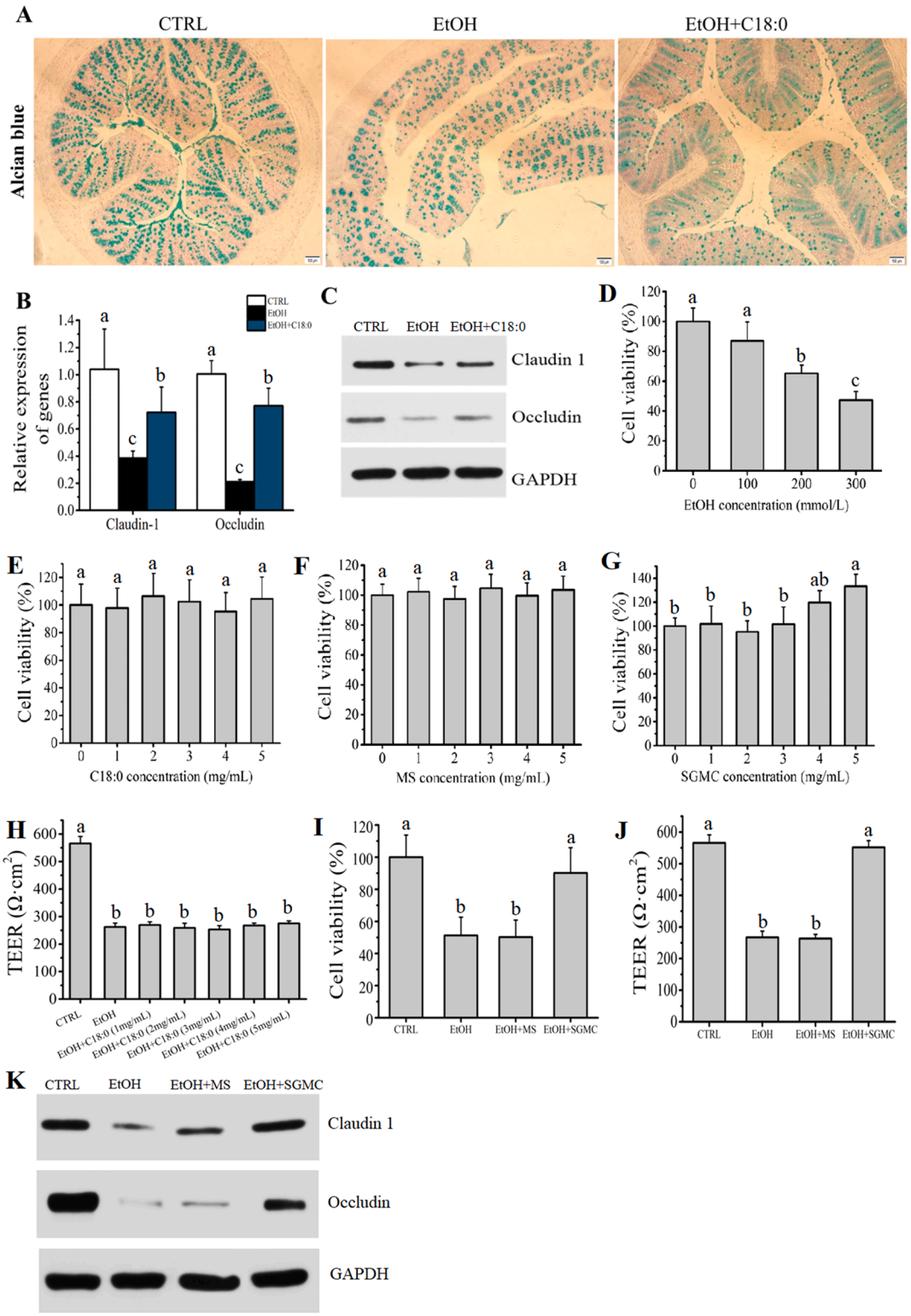

Fig. 6. Effects of stearic acid (C18:0) on intestinal barrier function in alcohol-treated mice. (A) Effect of stearic acid (C18:0) on colon mucus layer was stained with alcian blue in mice. (B) Effect of stearic acid (C18:0) on the mRNA expression levels of *Claudin-1* and *Occludin* in mice. (C) Effect of stearic acid (C18:0) on the protein expression levels of *Claudin-1* and *Occludin* in mice. (D) Effect of EtOH concentration on the level of cell viability on alcohol-induced Caco-2 cell injury model; (E) Effect of C18:0 concentration on the level of cell viability on alcohol-induced Caco-2 cell injury model; (F) Effect of MS concentration on the level of cell viability on alcohol-induced Caco-2 cell injury model; (G) Effect of SGMC concentration on the level of cell viability on alcohol-induced Caco-2 cell injury model; (H) Effect of stearic acid (C18:0) on the level of TEER on alcohol-induced Caco-2 cells injury model. (I) Effect of SGMC on the level of cell viability on alcohol-induced Caco-2 cells injury model. (J) Effect of SGMC on the level of TEER on alcohol-induced Caco-2 cells injury model. (K) Effect of SGMC on the protein expression levels of *Claudin-1* and *Occludin* on alcohol-induced Caco-2 cells injury model. Samples designated with different lower cases letters (a, b, c) were significantly different ($P < 0.05$) when compared different treatment group.

the viability of Caco-2 cell was not significantly decreased ($P > 0.05$) with the concentration of stearic acid (C18:0), MS and SGMC increasing, which confirmed that stearic acid (C18:0), MS and SGMC were not cytotoxic for Caco-2 cell. Therefore, the concentrations of alcohol (300 mmol/L), MS (5 mg/mL) and SGMC (5 mg/mL) were chosen for subsequent experiments. As shown in Fig. 6H, absolute stearic acid pretreatment could not protect the polarized Caco-2 cell monolayers from alcohol-induced damage. The results suggested that stearic acid could not improve intestinal TJs through direct interaction with intestinal epithelial cells. It is reasonable to speculate that the improvement in intestinal TJs is due to changes in the GM. To test this hypothesis, we investigated the effect of the supernatant from GM cultures (SGMC) on an alcohol-induced Caco-2 cell injury model in vitro. As shown in Fig. 6I-K, the absolute supernatant from cultures of the pretreated GM protected the polarized Caco-2 cell monolayers from alcohol-induced damage, which implied stearic acid ameliorates alcohol-induced intestinal barrier function disruption by altering the GM.

3.6. *Stearic acid ameliorated inflammatory responses in the livers of alcohol-treated mice*

LPS-mediated endotoxemia is considered to be an important factor in hepatitis caused by alcohol consumption (Leclercq, Matamoros, Cani, & Neyrinck, 2014). As shown in Fig. 7A, the levels of LPS in plasma were markedly increased after alcohol consumption, while stearic acid pretreatment significantly restrained this trend ($P < 0.05$). After alcohol consumption, the levels of the proinflammatory cytokines TNF-α, IL-1β and IL-6 were significantly ($P < 0.05$) increased in the liver and were associated with increased concentrations of LPS in the plasma (Fig. 7B). However, stearic acid pretreatment mitigated the increase in LPS-mediated proinflammatory cytokine levels. As shown in Fig. 7D, the levels of receptors (*TLR4*), coreceptors (*CD14* and *MD-2*) and adaptor molecules (*MyD88*) were significantly ($P < 0.05$) increased after alcohol consumption. Compared with the levels in the EtOH group, the levels of receptors (*TLR4*), coreceptors (*CD14* and *MD-2*) and adaptor molecules (*MyD88*) were significantly ($P < 0.05$) decreased in the stearic acid pretreatment group. *p-NF-kB/NF-kB* represents the phosphorylation level of *NF-kB* and is a marker of activation of the *NF-kB* signaling pathway. After alcohol consumption, the level of *p-NF-kB/NF-kB* was significantly ($P < 0.05$) increased, which indicated that the *NF-kB* signaling pathway was activated (Fig. 7C).

As a component of the cell wall of gram-negative bacteria, LPS is exposed to the gut when gram-negative bacteria die or dissolve (Hellman et al., 2000). Dysfunction of the intestinal barrier results in excess LPS being absorbed into the bloodstream and then, through portal vein circulation, being transported to the liver (Szabo, 2015). LPS is a major activator of Kupffer cells in the liver. When LPS binds to the *TLR4* receptor and coreceptors (*CD14* and *MD-2*), it recruits the connector molecule *MyD88*, which subsequently activates downstream signaling pathways. The *TLR4-MyD88* complex activates *NF-kB*, accelerates the

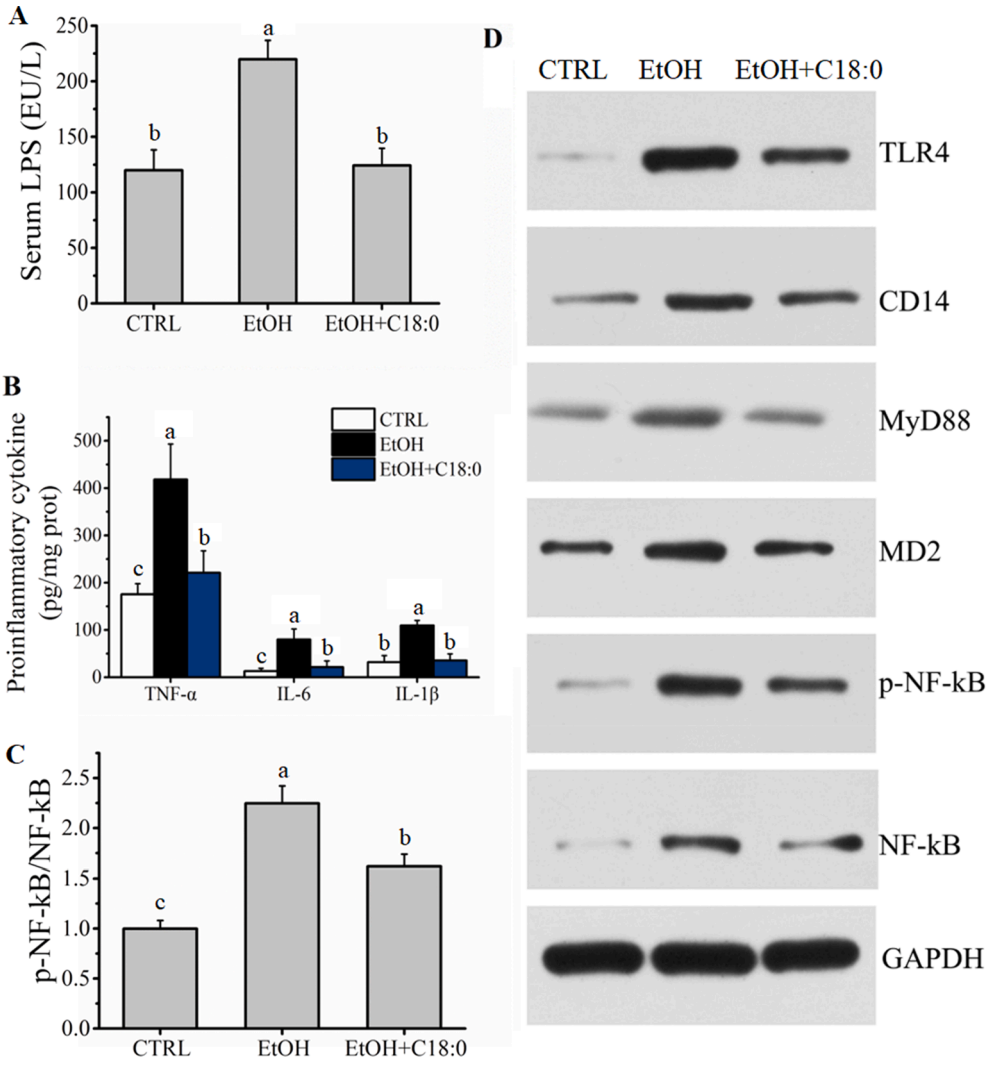

Fig. 7. Effects of stearic acid (C18:0) on inflammatory responses in alcohol-treated mice. (A) Effects of stearic acid (C18:0) on the levels of LPS in serum. (B) Effects of stearic acid (C18:0) on the levels of proinflammatory cytokine TNF-α, IL-1β and IL-6 in the liver. (C) The levels of *p-NF-kB p65/NF-kB p65* in hepatic (D) Effects of stearic acid (C18:0) on the levels of LPS receptors (*TLR4*), co-receptors (*CD14* and *MD2*) and *MyD88* in hepatic. Samples designated with different lower cases letters (a, b, c) were significantly different ($P < 0.05$) when compared different treatment group.

phosphorylation of *NF-kB*, and increases the production of proinflammatory cytokines, including IL-6, TNF-α, and IL-1, leading to liver inflammation (Cani, 2018). In this study, we found that stearic acid could enhance intestinal tight junction for reducing LPS leakage by regulating the abundance of *Akkermansia* and *Lactobacillus*, thereby inhibiting the expression of *LPS-TRL4* signaling pathway to prevent liver inflammation.

3.7. Stearic acid ameliorated oxidative stress in the livers of alcohol-treated mice

ROS-mediated oxidative stress is one of the important pathways of alcohol-induced liver damage (Zhu, Jia, Misra, & Li, 2012). In this study, the antioxidant enzymes (SOD and GSH-Px), oxidative stress factor (ROSs) and related signaling pathways (*CYP2E1*, *NRF2*, *HO-1*, AhR and NQO1) were investigated to determine whether the preventive effect of stearic acid is involved in the oxidative stress response. As shown in Fig. 8A, the oxidative stress factors ROS were significantly enriched after alcohol consumption compared with the level in the CTRL group ($P < 0.05$). However, stearic acid (C18:0) pretreatment significantly prevented the alcohol-induced increase in ROS levels ($P < 0.05$). Compared with the CTRL group, the activity of antioxidant enzymes (SOD (162.85 U/mg prot) and GSH-Px (46.31 U/mg prot)) were significantly decreased in the EtOH group ($P < 0.05$). Nevertheless, this trend was not reversed by stearic acid pretreatment (Fig. 8B). This confirmed that stearic acid prevented ROS production and was not involved in antioxidant enzyme (SOD and GSH-Px) activity. *CYP2E1* is an N-demethylase found mainly in the liver and has been confirmed to be key to promoting alcohol-induced oxidative stress by promoting ROS production (Nie et al., 2020). In contrast, the oxidation defense system of *NRF2/HO-1* and AhR/NQO1 were verified to play a key role in resisting ROS-mediated oxidative stress damage (Dong et al., 2021; Nie et al., 2020). As shown in Fig. 8C, the mRNA expression level of *CYP2E1* was significantly increased with alcohol treatment, whereas *HO-1*, *NRF2*, *AhR* and *NQO1* showed the opposite trend ($P < 0.05$). However, the mRNA expression level of *CYP2E1* was significantly ($P < 0.05$) decreased by stearic acid pretreatment but had no significant ($P > 0.05$) effect on *NRF2/HO-1*. Simultaneously, the mRNA expression level of *AhR* and *NQO1* were significantly increased with stearic acid pretreatment ($P < 0.05$). To confirm the regulatory mechanisms, changes in the proteins in the signaling pathway, including *AhR*, *NQO1* and *CYP2E1*, were assessed using western blot technique. Protein expression levels of *CYP2E1* were broadly raised, while in the alcohol-treated samples, the expression of *AhR* and *NQO1* decreased with alcohol-treated samples, which was similar to that of mRNA expression data. Nevertheless, this trend was reversed by stearic acid pretreatment (Fig. 8D). These results suggested that stearic acid ameliorated alcohol-induced oxidative stress damage mainly by inhibiting the expression of *CYP2E1* and activating *AhR/NQO1* signaling pathway to reduce the production of ROS but was not involved in the antioxidant defense system of *NRF2/HO-1*. Moreover, the accumulation of ROS is exacerbated by the translocation of LPS and the release of proinflammatory cytokines (Bala & Szabo, 2012). This is consistent with the results of this study.

3.8. Stearic acid ameliorated abnormal lipid metabolism in the livers of alcohol-treated mice

Abnormal lipid metabolism in the liver is one of the important characteristics of ALD (Crabb & Liangpunsakul, 2006). As shown in Fig. 9A-B, compared with the CTRL group, the levels of TG in plasma and liver were significantly increased after alcohol consumption. However, this trend was reversed by stearic acid pretreatment ($P < 0.05$). In addition, this result was further confirmed by histopathological examination of the liver (Fig. 9C). Hepatic transcriptional regulators are generally considered to be key factors regulating hepatic lipid synthesis (*SREBP1c*, *FAS* and *SCD1*) and output (*AMPK*, *PPARα* and *CPT1*) (Crabb & Liangpunsakul, 2006). As shown in Fig. 9D-E, the mRNA and protein expression levels of *SREBP1c*, *FAS* and *SCD1* were significantly increased after alcohol consumption, whereas the transcriptional regulators of *AMPK*, *PPARα* and *CPT1* showed the opposite trend ($P < 0.05$). Stearic acid pretreatment significantly ($P < 0.05$) inhibited alcohol-mediated elevation of *SREBP1c*, *FAS* and *SCD1* gene and protein expression

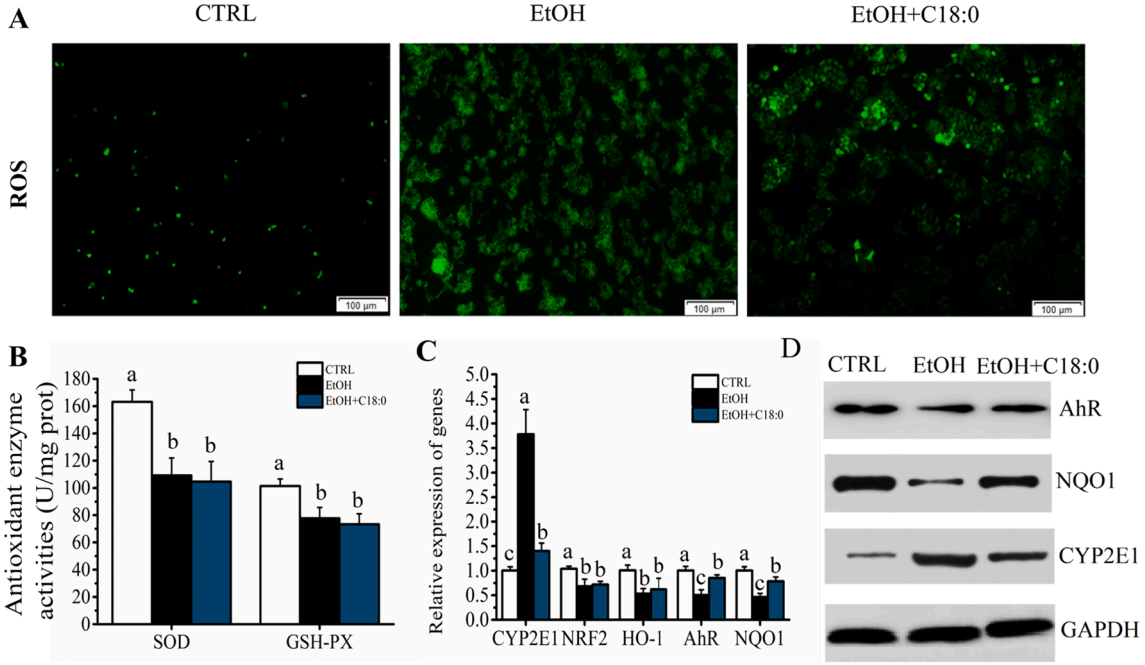

Fig. 8. (A) Effects of stearic acid (C18:0) on the levels of ROS in liver. (B) Effects of stearic acid (C18:0) on the levels of antioxidant enzyme activity in liver. (C) Effects of stearic acid (C18:0) on the mRNA expression levels of *CYP2E1*, *NRF2*, *HO-1*, *AhR* and *NQO1* in liver. (D) Effects of stearic acid (C18:0) on the protein expression levels of *CYP2E1*, *AhR* and *NQO1* in liver. Samples designated with different lower cases letters (a, b, c) were significantly different ($P < 0.05$) when compared different treatment group (same enzyme or gene).

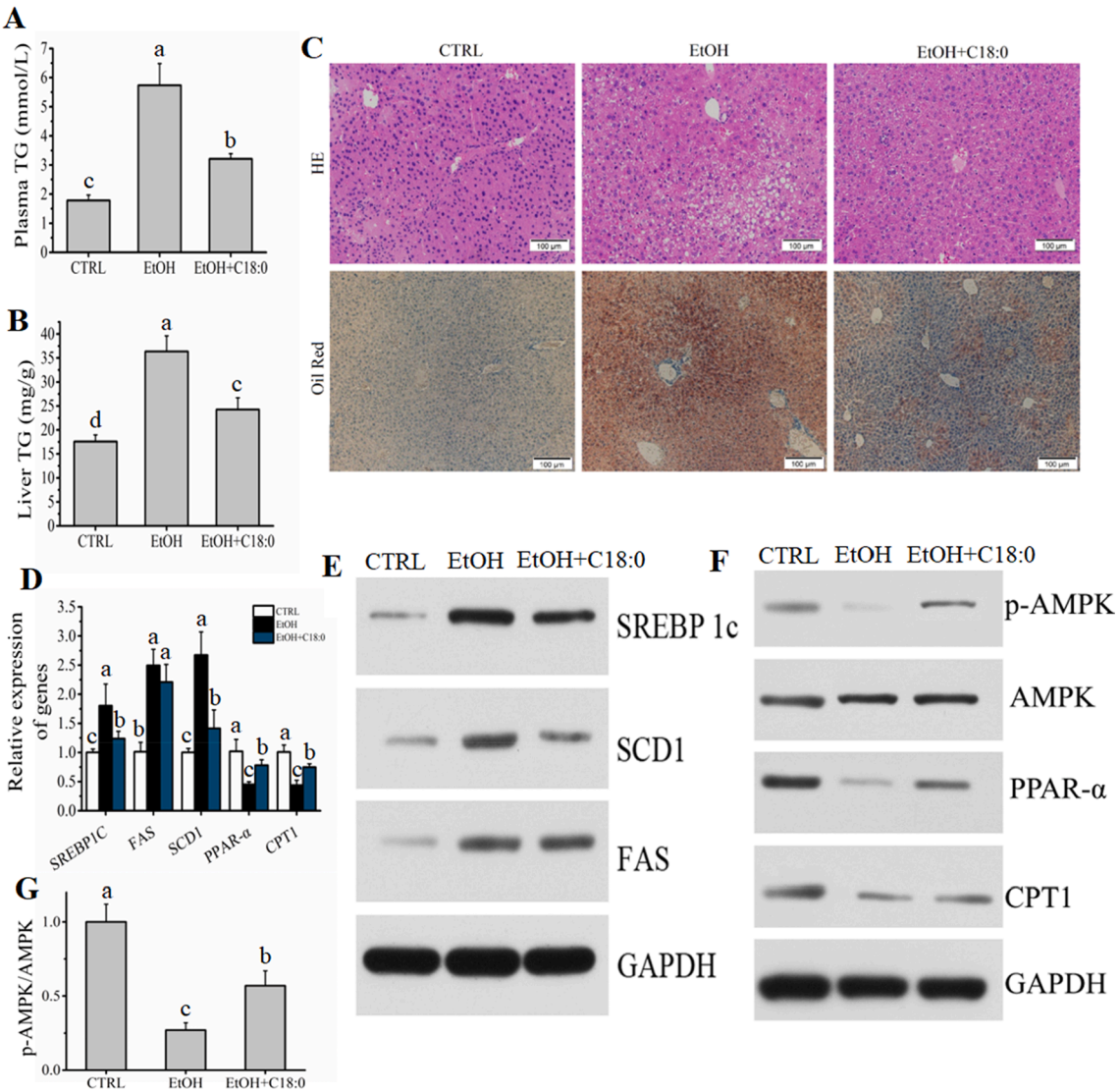

Fig. 9. (A) Effects of stearic acid (C18:0) on the levels of TG in plasma. (B) Effects of stearic acid (C18:0) on the levels of TG in liver. (C) Representative HE and Oil red staining of liver sections. (D) The expression levels of *SREBP1c*, *SCD1* and *FAS* genes in liver; (E-F) The mRNA and protein expression levels of *SREBP1c*, *SCD1*, *FAS*, *p-AMPK*, *AMPK*, *PPAR-α* and *CPT1* in liver. (G) The levels of *p-AMPK/AMPK* in liver. Samples designated with different lower cases letters (a, b, c) were significantly different ($P < 0.05$) when compared different treatment group.

(Fig. 9D-E). This suggests that stearic acid can inhibit alcohol-mediated liver lipid synthesis. Previous studies have confirmed that *AMPK*, *CPT1* and *PPARα* may function as central modulators of hepatic fat oxidation of the output, especially because *AMPK* activity is subject to the effects of ethanol (Tang, Lin, Lee, & Wang, 2014). After alcohol consumption, the *p-AMPK/AMPK* levels were significantly ($P < 0.05$) reduced, suggesting that alcohol significantly inhibited *AMPK* phosphorylation. In turn, the expression of *PPAR-α* and *CPT1* in downstream signaling pathways was significantly ($P < 0.05$) decreased, and liver lipid oxidation of the output was reduced (Fig. 9 D and F-G). This result is consistent with the above studies. However, stearic acid pretreatment significantly reversed this trend ($P < 0.05$). These results suggested that stearic acid pretreatment could significantly promote *AMPK* phosphorylation, activate the *AMPK* signaling pathway, promote the expression of the downstream *PPAR-α* and *CPT1* signaling pathways, and increase lipid oxidation in hepatocytes.

4. Conclusion

In conclusion, the mechanism underlying the prevention of ALD by stearic acid was ascribed to increasing relative abundances of *Akkermansia muciniphila* and *Lactobacillus* in the gut, which were beneficial to regulating intestinal homeostasis and ameliorating intestinal barrier dysfunction to reduce ROS-mediated oxidative stress damage and the LPS-mediated alcohol-associated hepatitis. This study demonstrated that dietary supplementation with saturated fatty acids could prevent or mitigate ALD by regulating the gut microbiota (GM) to reduce lipid synthesis and promote lipid oxidation output of liver. This study provides a more affordable dietary intervention strategy for the prevention of ALD.

Author contributions

Bao-cai Xu and Wen Nie proposed the project; Wen Nie and Fei-ran Xu designed the experiments; Wen Nie performed the experiments; Wen Nie, Fei-ran Xu and Kai Zhou wrote the manuscript; Xiao-xiao Yang, Hui Zhou and Bao-cai Xu revised and edited the manuscript.

CRediT authorship contribution statement

Wen Nie: Conceptualization, Methodology, Investigation, Writing – original draft. **Feiran Xu:** Writing – review & editing. **Kai Zhou:** Methodology, Investigation. **Xiaoxiao Yang:** Investigation. **Hui Zhou:** Writing – review & editing. **Baocai Xu:** Conceptualization, Supervision, Writing – review & editing.

Declaration of Competing Interest

The authors declare that they have no known competing financial interests or personal relationships that could have appeared to influence the work reported in this paper.

Acknowledgment

We would like to thank Drs. Ye-ye Du and Yuan-li Chen for providing us with the manuscript revision service. We would like to thank Suzhou BioNovo Gene Co., Ltd., for providing us with peptide mass spectrometry identification services.

Funding sources

This study was funded by major science and technology project of Anhui province (201903b06020004); natural science foundation of Anhui province (2008085QC144); special fund for Anhui province agricultural products processing industry technology system (340000211260001000420); the cooperation project from Anhui Qiangwang Flavouring Food Co., Ltd. (W2020JSKF0110); major science and technology projects of Anhui Province (202003b06020023 and 202003b06020022)

Appendix A. Supplementary material

Supplementary data to this article can be found online at https://doi.org/10.1016/j.foodres.2022.111095.

References

Albillos, A., de Gottardi, A., & Rescigno, M. (2020). The gut-liver axis in liver disease: Pathophysiological basis for therapy. *Journal of Hepatology, 72*, 558–577.

Arthur, I. C. (2006). Cytochrome P450 2E1-dependent oxidant stress and upregulation of anti-oxidant defense in liver cells. *Journal of Gastroenterology and Hepatology, 21*, 22–25.

Bala, S., & Szabo, G. (2012). Microrna signature in alcoholic liver disease. *International Journal of Hepatology*. https://doi.org/10.1155/2012/498232

Bertola, A., Mathews, S., Ki, S. H., Wang, H., & Gao, B. (2013). Mouse model of chronic and binge ethanol feeding (the niaaa model). *Nature Protocols, 8*, 627–637.

Brice, S., Julien, V., & Pedro, B. C. (2013). Role of AMPK activation in oxidative cell damage: Implications for alcohol-induced liver disease. *Biochemical Pharmacology, 86*, 200–209.

Cani, P. D. (2018). Human gut microbiome: Hopes, threats and promises. *Gut, 67*, 1716–1725.

Cone, R. A. (2009). Barrier properties of mucus. *Advanced Drug Delivery Reviews, 61*, 75–85.

Crabb, D. W., & Liangpunsakul, S. (2006). Alcohol and lipid metabolism. *Journal of Gastroenterology and Hepatology, 295*, 10–16.

Daglioglu, O., Tasan, M., & Tuncel, B. (2000). Determination of fatty acid composition and total trans fatty acids of Turkish biscuits by capillary gas-liquid chromatography. *European Food Research and Technology, 211*, 41–44.

Dong, H., Hao, L., Zhang, W., Zhong, W., Guo, W., Yue, R., et al. (2021). Activation of ahr-nqo1 signaling pathway protects against alcohol-induced liver injury by improving redox balance. *Cellular and Molecular Gastroenterology and Hepatology, 12*, 793–811.

Endo, M., Masaki, T., Seike, M., et al. (2007). TNF-α Induces Hepatic Steatosis in Mice by Enhancing Gene Expression of Sterol Regulatory Element Binding Protein-1c (SREBP-1c). *Experimental Biology and Medicine, 232*, 614–621.

Feng, R., Ma, L. J., & Wang, M. (2020). Oxidation of fish oil exacerbates alcoholic liver disease by enhancing intestinal dysbiosis in mice. *Communications Biology, 3*, 481–494.

Gao, B., & Bataller, R. (2011). Alcoholic liver disease: Pathogenesis and new therapeutic targets. *Gastroenterology, 141*, 1572–1585.

Grander, C., Adolph, T. E., Wieser, V., Lowe, P., Wrzosek, L., Gyongyosi, B., et al. (2018). Recovery of ethanol-induced Akkermansia muciniphila depletion ameliorates alcoholic liver disease. *Gut, 67*, 891–901.

Hellman, J., Loiselle, P. M., Tehan, M. M., Allaire, J. E., Boyle, L. A., & Kurnick, J. T. (2000). Outer membrane protein a, peptidoglycan-associated lipoprotein, and murein lipoprotein are released by escherichia coli bacteria into serum. *Infection and Immunity, 68*, 2566–2572.

Hsieh, P. S., Chen, C. W., Kuo, Y. W., & Ho, H. H. (2021). Lactobacillus spp. reduces ethanol-induced liver oxidative stress and inflammation in a mouse model of alcoholic steatohepatitis. *Experimental and Therapeutic Medicine, 21*, 1–9.

Huang, L. L., Wan, J. B., Wang, B., He, C. W., Ma, H., Li, T. W., et al. (2013). Suppression of acute ethanol-induced hepatic steatosis by docosahexaenoic acid is associated with downregulation of stearoyl-CoA desaturase1 and inflammatory cytokines. *Prostaglandins Leukotrienes and Essential Fatty Acids, 88*, 347–353.

Irina, K., Matthew, M., Matthew, C., Swati, J. B., & Craig, M. C. (2016). Alcoholic liver disease: Update on the role of dietary fat. *Biomolecules, 6*, 2–17.

Kirpich, I. A., Feng, W., Wang, Y., Liu, Y., Beier, J. I., Arteel, G. E., et al. (2013). Ethanol and dietary unsaturated fat (corn oil/linoleic acid enriched) cause intestinal inflammation and impaired intestinal barrier defense in mice chronically fed alcohol. *Alcohol, 47*, 257–264.

Leclercq, S., Matamoros, S., Cani, P. D., & Neyrinck, A. M. (2014). Intestinal permeability, gut-bacterial dysbiosis, and behavioral markers of alcohol-dependence severity. *Proceedings of the National academy of Sciences of the United States of America, 111*, 4485–4493.

Liu, Y., Luo, Y. K., Wang, X. H., Luo, L. Y., Sun, K., & Zeng, L. (2020). Gut Microbiome and Metabolome Response of Pu-erh Tea on Metabolism Disorder Induced by Chronic Alcohol Consumption. *Journal of Agricultural and Food Chemistry*. https://doi.org/10.1021/acs.jafc.0c01947

Louvet, A., & Mathurin, P. (2015). Alcoholic liver disease: Mechanisms of injury and targeted treatment. *Nature Reviews Gastroenterology & Hepatology, 12*, 231–242.

Macchione, I. G., Lopetuso, L. R., Ianiro, G., Napoli, M., Gibiino, G., Rizzatti, G., … Scaldaferri, F. (2019). Akkermansia muciniphila: key player in metabolic and gastrointestinal disorders. *European Review for Medical and Pharmacological Sciences, 23*, 8075–8083.

Massey, V. L., & Arteel, G. E. (2012). Acute alcohol-induced liver injury. *Front Physiol, 3*, 193–211.

Molina, P. E. (2008). Alcohol—intoxicating roadblocks and bottlenecks in hepatic protein and lipid metabolism. *American Journal of Physiology-endocrinology and Metabolism, 295*, E1–E2.

Nakajima, T., Kamijo, Y., Tanaka, N., Sugiyama, E., & Aoyama, T. (2010). Peroxisome proliferator-activated receptor alpha protects against alcohol-induced liver damage. *Hepatology, 40*, 972–980.

Nanji, A. A., & Frcnch, S. W. (1986). Dietary factors and alcoholic cirrhosis. *Alcoholism, Clinical and Experimental Research, 10*, 271–273.

Nanji, A. A., Griniuviene, B., Sadrzadeh, S. M., Levitsky, S., & McCully, J. D. (1995). Effect of type of dietary fat and ethanol on antioxidant enzyme mRNA induction in rat liver. *Journal of Lipid Research, 36*, 736–744.

Nanji, A. A., Mendenhall, C. L., & French, S. W. (1989). Beef fat prevents alcoholic liver disease in the rat. *Alcoholism, Clinical and Experimental Research, 13*, 15–19.

Nanji, A. A., Sadrzadeh, S. M., & Yang, E. K. (2010). Dietary saturated fatty acids: A novel treatment for alcoholic liver disease. *Alcoholism, Clinical and Experimental Research, 22*, 750–752.

Nanji, A. A., Zhao, S., Sadrzadeh, S. M., Dannenberg, A. J., Tahan, S. R., & Waxman, D. J. (1994). Markedly enhanced cytochrome P450 2E1 induction and lipid peroxidation is associated with severe liver injury in fish oil-ethanol-fed rats. *Alcoholism, Clinical and Experimental Research, 18*, 1280–1285.

Neyrinck, A. M., Etxeberria, U., Taminiau, B., Daube, G., Hul, M. V., & Everard, A. (2016). Rhubarb extract prevents hepatic inflammation induced by acute alcohol intake, an effect related to the modulation of the gut microbiota. *Molecular Nutrition & Food Research, 61*, 1–12.

Nie, W., Du, Y. Y., Xu, F. R., Zhou, K., Wang, Z. M., Dalali, S., et al. (2021). Oligopeptides from Jinhua ham prevent alcohol-induced liver damage by regulating intestinal homeostasis and oxidative stress in mice. *Food & Function*. https://doi.org/10.1039/D1FO01693H

Nie, W., Zhou, K., Wang, Y., Wang, Z. M., Xie, Y., Zhou, H., et al. (2020). Isolation and Identification of Bioactive Peptides from Xuanwei Hams Rescuing the Oxidative Stress Damage Induced by Alcohol in HHL-5 Hepatocytes. *Food & Function, 11*, 9710–9720.

Norberg, A., Jones, A. W., Hahn, R. G., & Gabrielsson, J. L. (2003). Role of variability in explaining ethanol pharmacokinetics: Research and forensic applications. *Clinical Pharmacokinetics, 42*, 1–31.

Pawlosky, R. J., Flynn, B. M., & Salem, N., Jr. (1997). The effects of low dietary levels of polyunsaturates on alcohol-induced liver disease in rhesus monkeys. *Hepatology, 26*, 1386–1392.

Pawlosky, R. J., & Salem, N., Jr. (2004). Development of alcoholic fatty liver and fibrosis in rhesus monkeys fed a low n-3 fatty acid diet. *Alcoholism, Clinical and Experimental Research, 28*, 1569–1576.

Peng, C., Torralba, M., Tan, J., Embree, M., & Schnabl, B. (2014). Supplementation of saturated long-chain fatty acids maintains intestinal eubiosis and reduces ethanol-induced liver injury in mice. *Gastroenterology, 148*, 203–214.

Rehm, J., Shield, K. D., Rehm, M. X., Gmel, G., & Frick, U. (2012). *Alcohol consumption, alcohol dependence, and attributable burden of disease in Europe: Potential gains from effective interventions for alcohol dependence*. Toronto, Canada: Centre for Addiction and Mental Health.

Room, R., Babor, T., & Rehm, J. (2005). Alcohol and public health. *Lancet, 365*, 519–530.

Saravanan, R., Viswanathan, P., & Pugalendi, K. V. (2006). Protective effect of ursolic acid on ethanol-mediated experimental liver damage in rats. *Life Sciences, 78*, 713–718.

Sarin, S. K., Pande, A., & Schnabl, B. (2019). Microbiome as a therapeutic target in alcohol-related liver disease. *Journal of Hepatology, 70*, 260–272.

Song, B. J., Moon, K. H., Olsson, N. U., & Salem, N., Jr. (2008). Prevention of alcoholic fatty liver and mitochondrial dysfunction in the rat by long-chain polyunsaturated fatty acids. *Journal of Hepatology, 49*, 262–273.

Szabo, G. (2015). Gut-live axis in alcoholic liver disease. *Gastroenterology, 148*, 30–36.

Tang, C. C., Lin, W. L., Lee, Y. J. Y. C., & Wang, C. J. (2014). Polyphenol-rich extract of Nelumbo nucifera leaves inhibits alcohol-induced steatohepatitis via reducing hepatic lipid accumulation and anti-inflammation in C57BL/6J mice. *Food & Funct, 5*, 678–687.

Tremaroli, V., & Bäckhed, F. (2012). Functional interactions between the gut microbiota and host metabolism. *Nature, 489*, 242–249.

Wada, S., Yamazaki, T., Kawano, Y., Miura, S., & Ezaki, O. (2008). Fish oil fed prior to ethanol administration prevents acute ethanol-induced fatty liver in mice. *Journal of Hepatology, 49*, 441–450.

Xia, T., Zhang, B., Li, S., Fang, B., Duan, W., Zhang, J., et al. (2020). Vinegar extract ameliorates alcohol-induced liver damage associated with the modulation of gut microbiota in mice. *Food & Funct, 11*, 2898–2909.

Xiao, C., Zhou, F., Zhao, M., Su, G., & Sun, B. (2018). Chicken breast muscle hydrolysates ameliorate acute alcohol-induced liver injury in mice through alcohol dehydrogenase (ADH) activation and oxidative stress reduction. *Food & Funct, 9*, 774–784.

Yan, A. W. (2012). Bacterial translocation and changes in the intestinal microbiome associated with alcoholic liver disease. *World. J. Hepatol, 4*, 110–118.

Yan, A. W., Fouts, D. E., Brandl, J., Stärkel, P., Torralba, M., Schott, E., et al. (2011). Enteric dysbiosis associated with a mouse model of alcoholic liver disease. *Hepatology, 53*, 96–105.

You, M. (2002). Ethanol Induces Fatty Acid Synthesis Pathways by Activation of Sterol Regulatory Element-binding Protein (SREBP). *Journal of Biological Chemistry, 277*, 29342–29347.

Zhu, H., Jia, Z., Misra, H., & Li, Y. R. (2012). Oxidative stress and redox signaling mechanisms of alcoholic liver disease: Updated experimental and clinical evidence. *J. Digest. Dis, 13*, 133–142.